Hittite Journal of Science and Engineering, 2018, 5 (1) 13-17
ISSN NUMBER: 2148-4171
DOI: 10.17350/HJSE19030000072

Cationic Dye Degradation by Means of an Efficient Photocatalyst Promoted by Aluminum Oxide

Kinyas Polat
Dokuz Eylul University, Department of Chemistry, Tınaztepe, Izmir, TURKEY..

Article History:
Received: 2017/08/25
Accepted: 2017/09/26
Online: 2017/12/28

***Correspondence to**: Kinyas Polat*
Department of Chemsitry, Dokuz Eylul University, Tınaztepe, Izmir, Turkey
Tel: +90 (232) 301-86 88
E-Mail: kinyas.polat@deu.edu.tr

ABSTRACT

A visible active magnetically separable two component MgFe2O4-Al2O3/Ag3VO4 photocatalyst was prepared in order to improve the catalytic activity of Ag3VO4 by utilizing Al2O3 (NPs Al2O3) adsorbent. Catalyst was characterized by using Fourier Transform Infrared spectrometer (FTIR). Photocatalytic activity of MgFe2O4-Al2O3/Ag3VO4 was measured by methylene blue (MB) degradation under visible light illumination emitted from 105 W tungsten light bulb. UV-vis spectrophotometer was employed to follow and identify the MB degradation and kinetics. Results suggested a first order kinetic model for the degradation having rate constant k, 0.03252 min-1. The half-life of catalytic degradation was found as 21.3 min. The photocatalytic activity of the neat Ag3VO4 was also measured and compared with the MgFe2O4-Al2O3/Ag3VO4. It was observed that rate constant of the degradation obtained with Ag3VO4 was 0.01577 min-1 and its half life 43.9 min. This revealed that an approximately twofold increase attained by using efficient nano Al2O3 adsorbent. At the end of the reaction catalyst particles were removed easily from the aqueous solution by a magnet.

Keywords:
Visible active photocatalyst, Methylene blue, Magnetic nanoparticle, First order kinetic, Degradation

INTRODUCTION

Rapid industrialization together with unconsciousness about environmental issues, business concerns and several other reasons prevent the factories to take robust preventing measures for released chemicals to water resources. This situation exposes extremely important health risk on the aquatic environment. Therefore, efficient technologies have to be employed to get rid of this problem. Recently photocatalytic degradation technologies by means of heterogeneous catalysis are of interest of the scientists. TiO_2 is the most heavily investigated photocatalysis to remove the dyes and other toxic chemicals from aqueous solutions up to now due to low cost, high chemical stability, high photoactivity and non-toxicity [1-3]. However, TiO_2 is only active under UV-light illumination which restricts to benefit from huge visible region of the solar spectrum because of its large band gap. Therefore, it is very important to develop photocatalysts sensitive to visible region. Several catalysts have been reported recently including $BiVO_4$, Bi_5O_7I/Bi_2O_3, g-C_3N_4/$BiOCl_xBr_{1-x}$, Ag/Ag_2CO_3-rGO, g-C_3N_4/WO_3 [4-9]. Among them Ag_3VO_4 attracts a lot of interest by scientist due to the appropriate band gap for the visible light adsorption, although photocatalytic activity of the catalyst is not sufficient due to the fast recombination. Recent efforts have been directed towards increasing the activity by using several strategies such as metal doping together with hybridizing [10-12], nanostructure engineering and using fast mediators such as graphene oxide and MoS_2 [13-15]. Other efficient strategy is combining photocatalytic material with a good adsorbent. By using this technique, the adsorption provides pre-concentration of molecules near the active sites of photocatalyst [16]. Other important issue in the heteregenous catalysis is the easy separation of catalyst from the medium without using conventional ways such as filtration and membrane separation. Therefore, recently $MgFe_2O_4$ nanoparticles have attracted interest of the scientist [17,18].

In this study magnetic $MgFe_2O_4$ particles and Al_2O_3 were used for the first time as an efficient adsorbent to improve the photocatlytic activity of Ag_3VO_4 in methylene blue degradation under visible light illumination from the aqueous solution.

MATERIALS AND METHODS

$FeCl_2.4H_2O$, $FeCl_3.6H_2O$, $Mg(OAc)_2.4H_2O$, NH_3 25 % solution and NaOH were taken from Merck. Al_2O_3, $AgNO_3$ and V_2O_5 were purchased from Aldrich.

Photocatalyst synthesis

V_2O_5 mixed with NaOH as 1:6 molar ratios in a round bottom flask by adding enough distilled water through continuous magnetic agitating. Then $AgNO_3$ solution was added resulting in yellow-orange precipitate. The related chemical reactions can be given as;

$$V_2O_5 + 6OH^- \xrightarrow{25\,°C} 2VO_4^{3-} + 3H_2O$$

$$3Ag^+ + VO_4^{3-} \xrightarrow{precipitation} Ag_3VO_4$$

The precipitate was left for 24 h at room temperature and washed with excess deionized water and dried at 70 °C. Calcination of the dried and cleaned precipitate was carried out at 300 °C for 4 h [19]. $MgFe_2O_4$ particles were synthesized by putting Al_2O_3 particles into the mixture of $FeCl_2.4H_2O$ and $FeCl_3.6H_2O$ in deionized water in oxygen-free Nitrogen atmosphere. Approximately 10 min later 25 % aqueous NH_3 (10 mL) was poured and stirred resulting in Fe_3O_4 particles. Co-precipitation occurred by subsequent drop wise addition of $Mg(OAc)_2.4H_2O$ to the suspension. $Mg(OH)_2$ was the final precipitate through addition of 1 M aqueous NaOH. The powder was cleaned with deionized water, filtered, dried and calcined at 550 °C for 6.5 h [20]. Subsequently, 0.5 g Ag_3VO_4 was blended with 0.5 % $MgFe_2O_4$-Al_2O_3 in an agate pestle for 30 min and calcined at 300 °C for 2 hours [21].

Photocatalytic performance evaluation

In order to determine the photocatalytic activity, MB solution including catalyst particles were illuminated under visible light of 105 W tungsten light bulb. MB concentration and the volume of the solution were $1x10^{-5}$ M and 50 mL. Photocatalyst was exposed to visible light at top of the continuously stirred beaker. Absorbance of the clear supernatants taken from the beaker at several time intervals was recorded at 664 nm wavelength by using a UV-visible spectrophotometer.

RESULTS AND DISCUSSION

Photocatalytic degradation mechanism

MB degradation or oxidation by visible light in the presence of a photocatalysis takes place mainly due to the creation of active species, such as peroxyl and hydroxyl radicals. By the attack of these radicals, MB molecule is mineralized into nontoxic products [22, 23]. A general mechanism reported frequently [23] can be given below;

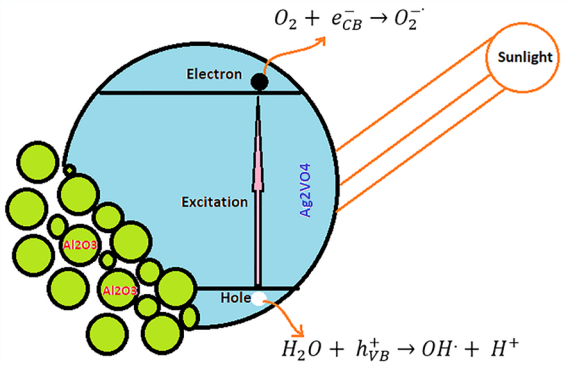

Figure 1. Schematic representation of a degradation mechanism of MB under visible light

$$Catalyst + h\gamma \xrightarrow{excitation} \left(e_{CB}^- + h_{VB}^+\right)$$
$$H_2O + h_{VB}^+ \rightarrow OH^{\cdot} + H^+$$
$$O_2 + e_{CB}^- \rightarrow O_2^-$$
$$O_2^- + H_2O \rightarrow H_2O_2$$
$$OH^{\cdot}\ or\ HOO^{\cdot} + MB \xrightarrow{degradation} inorganic\ degradation\ products\ of\ MB$$

The reaction mechanism that converts MB into final products may be represented as in the Figure 1.

Kinetics of photocatalysis

Langmuir–Hinshelwood (L–H) model is generally fitted to derive the kinetic model of the photocatalysis reactions. If MB concentration is maintained at low levels, degradation usually follows first order kinetic model [24, 25]. L-H kinetic expression is given in the equation 1.

$$r = \frac{dC}{dt} = \frac{kKC}{1 + KC} \quad (1)$$

In the L-H equation, r is the observed reaction rate, k is the intrinsic reactivity constant, K is the equilibrium adsorption constant, C is the reactant concentration. L-H expression can be reduced to first order kinetic equation for dilute solutions (1+KC equals to 1);

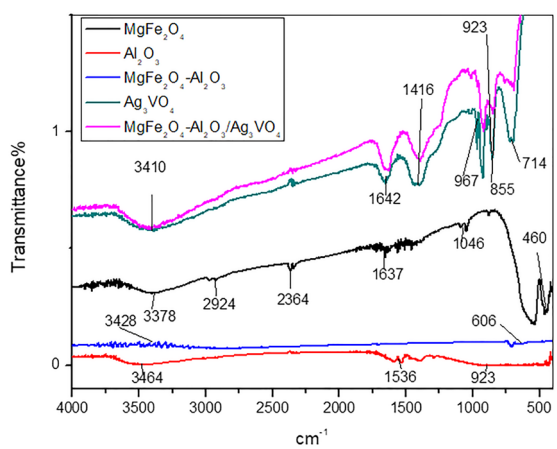

Figure 2. FTIR spectrums for $MgFe_2O_4$-Al_2O_3/Ag_3VO_4 and its individual ingredients

$$r = \frac{dC}{dt} = -k_g C \quad (2)$$

Integrating the equation 2 from C to C_0 (initial concentration of the dye) gives the linear relation of first order kinetic equation;

$$\ln\left(\frac{C}{C_0}\right) = -k_g t \quad (3)$$

C is the concentration of MB at time t, k_g is the observed rate constant. A plot of $\ln(C/C_0)$ versus t produces a linear relationship, the slope gives the observed rate constant, k_g. Half-life of the degradation is calculated by;

$$[\text{Ochratoxin A}]\left(\frac{\mu g}{ml}\right) = \frac{\text{Abs}(333\,\text{nm}) \times \text{Molecular Weight} \times 1000}{\text{Ochratoxin A Extinction Coefficient}} = \frac{\text{Abs}(333\,\text{nm}) \times 403 \times 1000}{5550} = \text{Abs}(333\,\text{nm}) \times 72.6 \quad (4)$$

Structural identity by FTIR

FTIR spectrums were collected as 50 scans at 4cm^{-1} resolution between 4000 and 400 cm^{-1} with a Perkin Elmer Spectrum BX-II FTIR spectrometer.

The absorption bands (Figure 2) at 3464-3378 cm^{-1} and 1637 cm^{-1} are due to the O-H stretching vibration of H_2O remaining after calcination. 2924 cm^{-1} and 1046 cm^{-1} represent the stretching and bending vibrations of C-H as impurities. The peak at 2364 cm^{-1} stands for the CO_2 in the air [26]. Specific bands observed at 606 and 460 cm^{-1} correspond to the metal-oxygen bonds in the tetrahedral and octahedral sites and suggest that $MgFe_2O_4$ has spinel structure [27-29]. In the spectrum of $MgFe_2O_4$/NPs-Al_2O_3 metal-oxygen band intensities showed a clear decrease. In the FTIR spectrum of Ag_3VO_4, 714 cm^{-1}, 855 cm^{-1}, 923 cm^{-1} and 967 cm^{-1} bands are due to the Ag_3VO_4. Absorptions at 923 cm^{-1} and 967 cm^{-1} represent the symmetric vibrations and 855 and 714 cm^{-1} represent the asymmetric stretching vibrations of V-O bonds in VO_3, respectively.

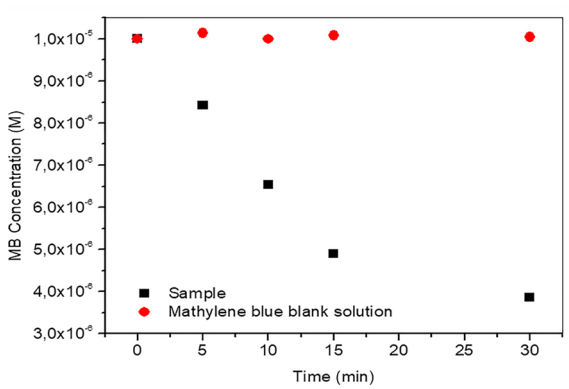

Figure 3. Decreasing MB concentration upon irradiation of $MgFe_2O_4$-Al_2O_3/Ag_3VO_4 with visible light

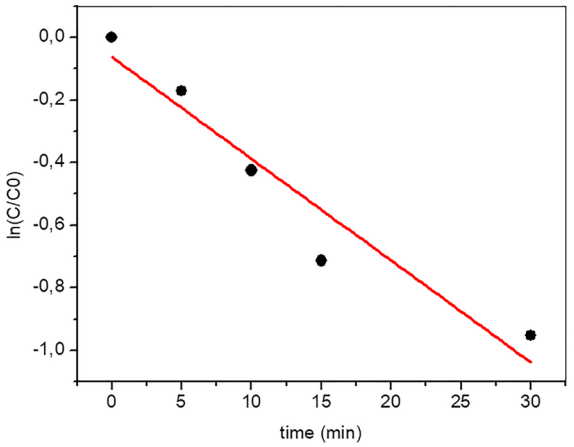

Figure 4. First order kinetic model fitting of MB degradation with $MgFe_2O_4$-Al_2O_3/Ag_3VO_4

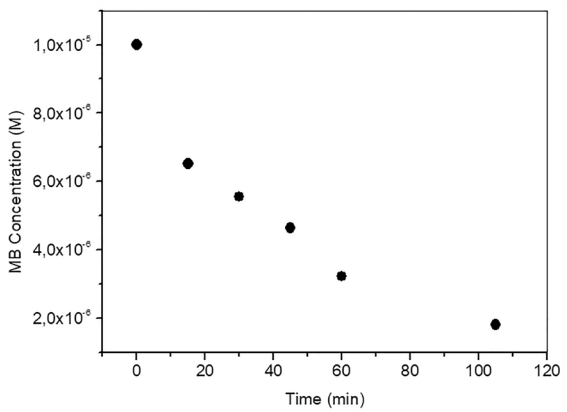

Figure 5. Decreasing MB concentration upon irradiation of Ag_3VO_4 with visible light

The absorption at 1416 cm^{-1} is due to the overtone. Since the amount of $MgFe_2O_4$-Al_2O_3 is 0.5 %, no difference was recorded between the FTIR spectrum of Ag_3VO_4 and $MgFe_2O_4$-Al_2O_3/Ag_3VO_4.

MB photocatalytic degradation

Photocatalytic MB degradation performance of $MgFe_2O_4$-Al_2O_3/Ag_3VO_4 was tested under visible light source. Remaining dye concentration in the aqueous solution upon interaction with light was measured by UV-vis spectrophotometer at 664 nm where the dye absorption reaches a maximum. The initial MB concentration was 1x10^{-5} M. The catalyst weight was 0,1 g. The change of MB degradation with time (Figure 3) suggests that an efficient reaction takes place upon irradiation with fast reduction in concentration of MB. Kinetic model of the degradation as seen from Figure 4 obeys to first order kinetics. Rate constant k was found to be 0,03252 min^{-1} and corresponding half-life which MB concentration decreases to half of its initial value is 21.3 min. During the experiment a methylene blue witness sample at the same concentration was placed near the main sample to

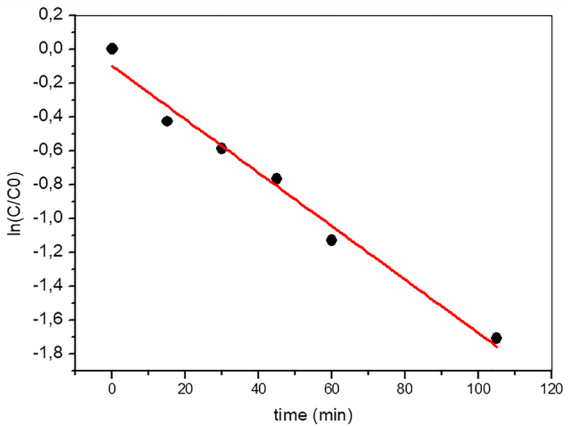

Figure 6. First order kinetic model fitting of MB degradation with Ag_3VO_4

indicate whether the experimental conditions have effect on the degradation. As seen from the Figure 4, MB blue concentration does not change during the experiment verifying that without catalyst no degradation occurs that stem from the experimental conditions.

For evaluating the effect of Al_2O_3 to the catalytic performance Ag_3VO_4 was tested separately. The change of MB concentration with time was given in Figure 5. The change of $\ln(C/C_0)$ with time was also given in Figure 6 to identify the rate constant of degradation. It is clear that MB blue degradation with Ag_3VO_4 lasts longer than that of $MgFe_2O_4$-Al_2O_3/Ag_3VO_4 when Figures 3 and Figure 5 are compared. Figure 6 suggest that degradation kinetics correspond to first order model again. Rate constant of the degradation with Ag_3VO_4 was 0,01577 min^{-1}. Half life was found as 43.9 min.

From the degradation half-lives which are 21.3 min for $MgFe_2O_4$-Al_2O_3/Ag_3VO_4 and 43.9 min for Ag_3VO_4, it is clear that incorporating Al_2O_3 particles to the Ag_3VO_4 acted positively to enhance the photocatalytic activity at least twofold when compared to neat Ag_3VO_4. This effect can be attributed to the adsorption of dye molecules by Al_2O_3. By the help of this adsorption, a pre-concentration of dye molecules near the catalyst is created which accordingly increases the rate of reaction [16]. A photograph of MB degradation with $MgFe_2O_4$-Al_2O_3/Ag_3VO_4 photocatalyst is given in the Figure 7.

The photograph (Figure 7) shows that how efficient does MB degradation take place in the presence of a photocatalyst under visible light. It is also seen that after the completion of reaction, catalyst particles consist of $MgFe_2O_4$ magnetic particles are easily attracted by a magnet without needing extra filtration step.

CONCLUSION

In this study visible active, magnetic $MgFe_2O_4$-Al_2O_3/Ag_3VO_4 photocatalyst was successfully synthesized and tested against MB degradation under visible light illumination by 105 W tungsten light bulb. The study showed that adsorbent (Al_2O_3 particles) adding strategy produced positive result in enhancing the photocatalytic activity of Ag_3VO_4 almost twofold. Reaction rate as inferred from the half life time of degradation with $MgFe_2O_4$-Al_2O_3/Ag_3VO_4 catalyst which is 21.3 min was nearly half of that (43.9 min) with neat Ag_3VO_4. Corresponding reaction rate constants, k for $MgFe_2O_4$-Al_2O_3/Ag_3VO_4 and Ag_3VO_4 were identified as 0.03252 min^{-1} and 0.01577 min^{-1}, respectively. The kinetic model of the MB degradation by these catalyst was well fitted by first order kinetics. The catalyst introduced in this study proved that it can be removed easily from the aqueous solution by a magnet bar due to the magnetic particles of $MgFe_2O_4$ eliminating the difficult conventional separation techniques.

ACKNOWLEDGEMENTS

I want to thank Prof.Dr.Mürüvvet Yurdakoc for valuable helps and to her MSc student Yıldıray Aldemir.

REFERENCES

1. Harraz FA, Abdel-Salam OE, Mostafa AA, Mohamed RM, Hanafy M. Rapid synthesis of titania-silica nanoparticles photocatalyst by a modified sol-gel method for cyanide degradation and heavy metals removal. Journal of Alloys

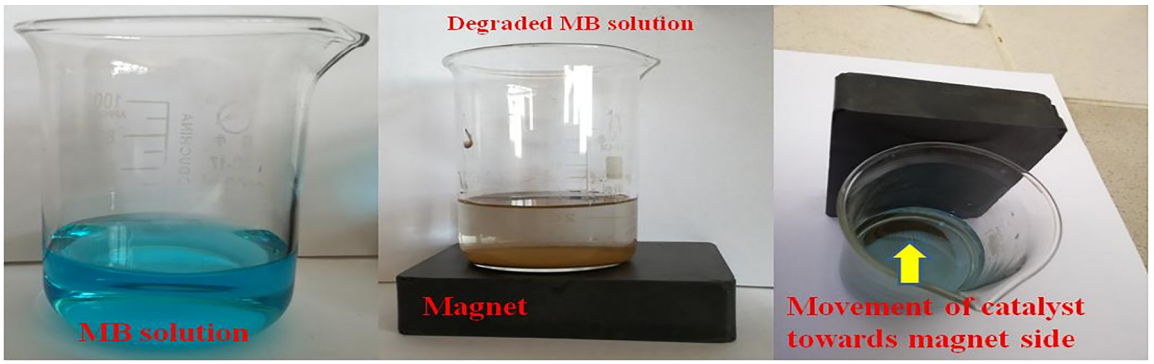

Figure 7. Photograph of the MB degradation steps under visible light

and Compounds 551 (2013) 1–7.
2. El–Toni AM, Yin S, Sato T, Ghannam T, Al–Hoshan M, Al–Salhi M. Investigation of photocatalytic activity and UV–shielding properties for silica coated titania nanoparticles by solvothermal coating. Journal of Alloys and Compounds 508 (2010) L1–L4.
3. Abbasi A, Ghanbari D, Salavati–Niasari M, Hamadanian M. Photo–degradation of methylene blue: photocatalyst and magnetic investigation of Fe_2O_3-TiO_2 nanoparticles and nanocomposites. Journal of Materials Science: Materials in Electronics 27 (5) (2016) 4800–4809.
4. Guo M, Qianglong H, Wenjie W, Jie W, Weimin W. Fabrication of $BiVO_4$: Effect of structure and morphology on photocatalytic activity and its methylene blue decomposition mechanism, Journal of Wuhan University of Technology–Materials Science Education 31 (4) (2016) 791–798.
5. Umaporn L, Khatcharin W, Sukon P, Wiyong K, Natda W. $InVO_4$-$BiVO_4$ composite films with enhanced visible light performance for photodegradation of methylene blue. Catalysis Today 278 (2) (2016) 291–302.
6. Cheng L, Kang Y. Bi_5O_7I/Bi_2O_3 composite photocatalyst with enhanced visible light photocatalytic activity. Catalyst Communucations 72 (2015) 16–19.
7. Shi S, Gondal MA, Rashid SG, Qi Q, Al–Saadi AA, Yamani ZH. Synthesis of g–$C_3N_4/BiOCl_xBr_{1+x}$ hybrid photocatalysts and the photoactivity enhancement driven by visible light. Colloids Surface A: Physicochemical Engineering Aspects 461 (2014) 202–11.
8. Song S, Chenga B, Wu N, Meng A, Cao S, Yu J. Structure effect of graphene on the photocatalytic performance of plasmonic Ag/Ag_2CO_3–rGO for photocatalytic elimination of pollutants. Applied Catalysis B: Environmental 181 (2016) 71–78.
9. Jin Z, Murakami N, Tsubota T, Ohno T. Complete oxidation of acetaldehyde over a composite photocatalyst of graphitic carbon nitride and tungsten(VI) oxide under visible–light irradiation. Applied Catalysis B: Environmental 150–151 (2014) 479–485.
10. Mohsen P. Visible–light photoactive Ag-AgBr/α–Ag_3VO_4 nanostructures prepared in a water–soluble ionic liquid for degradation of wastewater. Applied Nanoscience 6 (2016), 1119–1126.
11. Ming Y, Yilin W, Yan Y, Xu Y, Fangfang Z, Yinqun H, and Weidong S. Synthesis and Characterization of Novel $BiVO_4/Ag_3VO_4$ Heterojunction with Enhanced Visible–Light–Driven Photocatalytic Degradation of Dyes. ACS Sustainable Chemistry & Engineering 4 (3) (2016) 757–766.
12. Hui X, Huaming L, Li X, Chundu W, Guangsong S, Yuanguo X, Jinyu C. Enhanced Photocatalytic Activity of Ag_3VO_4 Loaded with Rare–Earth Elements under Visible–Light Irradiation. Industrial Engineering Chemistry Research 48 (24) (2009) 10771–10778.
13. Lei G, Zhonghua L, Jiawen L. Facile synthesis of Ag_3VO4/β–$AgVO_3$ nanowires with efficient visible–light photocatalytic activity. RSC Advances 7 (2017) 27515–27521.
14. Tingting Z, Liying H, Yanhua S, Zhigang C, Haiyan J, Yeping L, Yuanguo X, Qi Z, Hui X, Huaming L. Modification of Ag_3VO_4 with graphene–like MoS_2 for enhanced visible–light photocatalytic property and stability. New Journal of Chemistry 40 (2016) 2168–2177.
15. Ran R, Meng XC, Zhang ZS, Facile preparation of novel graphene oxide–modified $Ag_2O/Ag_3VO_4/AgVO_3$ composites with high photocatalytic activities under visible light irradiation. Applied Catalysis B: Environmental 196 (2016) 1–15.
16. Carl A, Allen JB. Improved Photocatalytic Activity and Characterization of Mixed TiO_2/SiO_2 and TiO_2/Al_2O_3 Materials. Journal of Physical Chemistry B 101 (1997) 2611–2616.
17. Iliya A, Maryam M, Nahid R. $MgFe_2O_4$ and $MgFe_2O_4/ZnFe_2O_4$ coated with polyaniline as a magnetically separable photocatalyst for removal of a two dye mixture in aqueous solution. Research on Chemical Intermediates 43 (2017) 4459–4474.
18. Nabiyouni G, Ghanbari D, Ghasemi J, Yousofnejad A. Microwave–assisted Synthesis of $MgFe_2O_4$–ZnO Nanocomposite and Its Photocatalyst Investigation in Methyl Orange Degradation. Journal of Nano Structures 5(3) (2015) 289–295.
19. Wang J, Wang P, Cao Y, Chen J, Li W, Shao Y, Zheng Y, Li D. A high efficient photocatalyst Ag_3VO_4/TiO_2/graphene nanocomposite with wide spectral response. Applied Catalysis B. Environmental 136–137 (2013) 94–102.
20. Sheykhan M, Mohammadnejad H, Akbari J, Heydari A. Superparamagnetic magnesium ferrite nanoparticles: a magnetically reusable and clean heterogeneous catalyst. Tetrahedron Letters 53 (2012) 2959–2964.
21. Zhang L, He Y, Ye P, Wu T, Enhanced photodegradation activity of Rhodamine B by $MgFe_2O_4/Ag_3VO_4$ under visible light irradiation. Catal Communications 30 (2013) 14–18.
22. Phaltane AS, Vanalakar SA, Bhat TS, Patil PS, Sartale SD, Kadam LD. Photocatalytic degradation of by hydrothermally synthesized CZTS nanoparticles. Journal of Materials Science: Materials in Electronics 28 (2017) 8186–8191.
23. Hassena H. Photocatalytic Degradation of by Using Al_2O_3/Fe_2O_3 Nano Composite under Visible Light. Modern Chemistry & Applications 4(1) (2016) 1–5.
24. Khataee AR, Fathinia M, Aber S. Kinetic Modeling of Liquid Phase Photocatalysis on Supported TiO_2 Nanoparticles in a Rectangular Flat–Plate Photoreactor. Industrial Engineering and Chemistry Research 49 (2010) 12358–12364.
25. Jiamei W, Can L, Hong Z, Jianhao Z. Photocatalytic degradation of methylene blue and inactivation of gram–negative bacteria by TiO_2 nanoparticles in aqueous suspension. Food Control 34 (2013) 372–377.
26. Yıldıray A, Magnetik özellikli taşıyıcılı nanokatalizörlerin hazırlanması ve karakterizasyonu, Yüksek Lisans Tezi, Dokuz Eylül Üniversitesi, İzmir, 2016.
27. Sheykhan M, Mohammadnejad H, Akbari J, Heydari A. Superparamagnetic magnesium ferrite nanoparticles: A magnetically reusable and clean heterogeneous catalyst. Tetrahedron Letters 53 (2012) 2959–2964.
28. Khot VM, Salunkhe AB, Thorat ND, Phadatare MR, Pawar SH. Induction heating studies of combustion synthesized $MgFe_2O_4$ nanoparticles for hyperthermia applications. Journal of Magnetism and Magnetic Materials 332 (2013) 48–51.
29. Hoque SM, Hakim MA, Mamun A, Akhter S, Hasan MT, Paul DP. Study of the bulk magnetic and electrical properties of $MgFe_2O_4$ synthesized by chemical method. Materials Sciences and Applications 2 (2011) 1564.